AIAA SciTech Forum
9 - 13 January 2017, Grapevine, Texas
58th AIAA/ASCE/AHS/ASC Structures, Structural Dynamics, and Materials Conference
10.2514/6.2017-0134

Automated Selection of Low-Fidelity Models for Rapid Aerodynamic Shape Optimization Using Physics-Based Surrogates

Slawomir Koziel[1]
Engineering Optimization & Modeling Center, Reykjavik University, Menntavegur 1, 101 Reykjavik, Iceland

Leifur Leifsson[2], and Anand Amrit[3]
Iowa State University, Ames, Iowa, 50011

Physics-based surrogate models require the selection and setup of fast low-fidelity models, and their subsequent alignment with the computationally expensive high-fidelity models. A technique for automated low-fidelity model setup is proposed. The technique exploits statistical analysis of low- and high-fidelity model misalignments conducted using several reference designs allocated in the search space. The paper demonstrates that the technique permits selection of a suitable low-fidelity model which translates into improved performance of the optimization algorithm. For illustration purposes, lift-constrained drag minimization of transonic airfoils is considered. The results indicate that an appropriate selection of a low-fidelity model allows for a reduction in the cost of the optimization without the risk of failure due to insufficient model accuracy.

I. Introduction

Aerodynamic shape optimization using high-fidelity computational fluid dynamics (CFD) simulation models can be accelerated using surrogate-based optimization[1] (SBO). In particular, SBO using physics-based surrogate models have been demonstrated to be very efficient.[2,3] Those types of surrogates are typically constructed using a response corrected low-fidelity model. The purpose of the response correction is to align the low-fidelity models with the high-fidelity ones. The selection and setup of the low-fidelity models is currently a hands-on process. Moreover, it is not clear how the low-fidelity model should be setup so the performance of the optimization process is improved. This paper proposes a technique for automated low-fidelity model setup by examining the misalignment and selecting the ones that provide an acceptable correlation with the high-fidelity model. The technical details of the approach are provided in the paper, along with an illustration on a design problem involving aerodynamic shape optimization of airfoils in inviscid transonic flow.

II. Methodology

A. Surrogate-based Optimization

Constrained nonlinear minimization of the following form is considered[2]

$$\mathbf{x}^* = \arg\min_{\mathbf{l}\le\mathbf{x}\le\mathbf{u}} H(\mathbf{f}(\mathbf{x})) \text{ s.t. } \mathbf{g}(\mathbf{x})\le 0,\ \mathbf{h}(\mathbf{x})=0, \tag{1}$$

where $\mathbf{x}$ is the design variable vector, $\mathbf{x}^*$ is the optimized design, H is a scalar valued objective function, $\mathbf{f}(\mathbf{x})$ is a vector with the figures of merit, $\mathbf{g}(\mathbf{x})$ is a vector with the inequality constraints, $\mathbf{h}(\mathbf{x})$ is a vector with the equality constraints, and $\mathbf{l}$ and $\mathbf{u}$ are the lower and upper bounds of $\mathbf{x}$, respectively. It is assumed the vectors $\mathbf{f}$, $\mathbf{g}$, and $\mathbf{h}$ are derived from high-fidelity PDE simulations.

Solving (1) is accelerated by surrogate-based modeling and optimization within a trust region framework[2]

$$\mathbf{x}^{(i+1)} = \arg\min_{\mathbf{x},\ \|\mathbf{x}-\mathbf{x}^{(i)}\|\le\delta^{(i)}} H(\mathbf{s}^{(i)}(\mathbf{x})), \tag{2}$$

[1] Professor, School of Science and Engineering, Senior Member AIAA.
[2] Assistant Professor, Department of Aerospace Engineering, Senior Member AIAA.
[3] Graduate Student, Department of Aerospace Engineering, Student Member AIAA.

where $\mathbf{x}^{(i)}$, $i = 0, 1, \ldots$, is a sequence of approximate solutions to (1), $\mathbf{s}^{(i)}(\mathbf{x})$ is a surrogate model of $\mathbf{f}(\mathbf{x})$ at iteration i, and $\delta^{(i)}$ is the trust region search radius[4] at iteration i.

B. Physics-based Aerodynamic Surrogate Models via Multi-point Output Space Mapping

Multi-point output space mapping[2] (OSM) is utilized to construct the aerodynamic surrogate models as

$$\mathbf{s}^{(i)}(\mathbf{x}) = \mathbf{A}^{(i)} \circ \mathbf{c}(\mathbf{x}) + \mathbf{D}^{(i)} + \mathbf{q}^{(i)}, \tag{3}$$

where $\mathbf{c}(\mathbf{x})$ is a vector with the figures of merit obtained from a model of lower fidelity than $\mathbf{f}(\mathbf{x})$ (see Sect. II.C), and $\mathbf{A}^{(i)}$ and $\mathbf{D}^{(i)}$ are global response correction parameters, and $\mathbf{q}^{(i)}$ is a local response correction parameter. In general, the global parameters are obtained by solving[2]

$$[\mathbf{A}^{(i)}, \mathbf{D}^{(i)}] = \arg\min_{[\mathbf{A},\mathbf{D}]} \sum_{k=0}^{i} \| \mathbf{f}(\mathbf{x}^{(k)}) - (\mathbf{A} \circ \mathbf{c}(\mathbf{x}^{(k)}) + \mathbf{D}) \|^2 \cdot \tag{4}$$

However, to avoid solving this nonlinear minimization problem the global parameters are obtained by solving a linear regression problem equivalent to (4) using a least-square optimal solution. The details of the calculation can be found in Leifsson and Koziel[3]. The local parameter is defined as[2]

$$\mathbf{q}^{(i)} = \mathbf{f}(\mathbf{x}^{(i)}) - [\mathbf{A}^{(i)} \circ \mathbf{c}(\mathbf{x}^{(i)}) + \mathbf{D}^{(i)}]. \tag{5}$$

In this work, the solution of algorithm (2) with the surrogate model (3) is carried out using the pattern search algorithm[4], and the termination condition is the one that occurs first during the optimization run of the following criteria: $\|\mathbf{x}^{(i)} - \mathbf{x}^{(i-1)}\| < \varepsilon_x$, $|H^{(i)} - H^{(i-1)}| < \varepsilon_H$, and $\delta^{(i)} < \varepsilon_\delta$, where $\varepsilon_x = 10^{-3}$, $\varepsilon_H = 10^{-4}$, and $\varepsilon_\delta = 10^{-3}$ are the convergence tolerances.

C. Automated Low-fidelity Model Selection by Statistical Analysis

A simple technique is proposed that allows for estimating the high- and low-fidelity model correlations through statistical analysis executed for a set of reference designs. The method works as follows. Let $\mathbf{x}^{(k)}$, $k = 1, 2, \ldots, K$, be a set of reference designs such that both the high- and low-fidelity models evaluations are available at all $\mathbf{x}^{(k)}$. All pairs of designs $\{\mathbf{x}^{(k)},\mathbf{x}^{(j)}\}$, $k, j = 1, \ldots, K$, are considered such that $k \neq j$, and corresponding differences

$$df_{qkj} = f_q(\mathbf{x}^{(k)}) - f_q(\mathbf{x}^{(j)}), \tag{6}$$

$$dc_{qkj} = c_q(\mathbf{x}^{(k)}) - c_q(\mathbf{x}^{(j)}), \tag{7}$$

where f_q and c_q are the elements q-th elements, where $q = 1,\ldots,N$, of the vectors $\mathbf{f}$ and $\mathbf{c}$, respectively. Here, the reference designs are split into groups of clusters (three designs in each cluster). The differences (6), (7) are only calculated within the clusters. Thus, the total number of pairs (6) is $3K$.

In the next step, linear regression models are calculated for the data sets $\{df_{qkj},dc_{qkj}\}$, and the coefficient of determination r^2 is computed, which describes how well the low- and high-fidelity data sets are correlated. Note that $r^2 = 1.0$ corresponds to a perfect correlation, and $r^2 = 0.0$ corresponds to no correlation. Here, $r^2 = 0.9$ is used as a satisfactory correlation level.

III. Numerical Study

A. Description

The numerical study considers airfoil shape optimization, and is in two parts. The correlations of the high- and low-fidelity models are studied by varying the computational discretization using the proposed statistical analysis approach (as described in Sect. II.C). The results are validated by solving the optimization problem several times using multi-point OSM (as described in Sect. II.B) with the high-fidelity model and each low-fidelity model.

The problem involves lift-constrained drag minimization of the RAE 2822 in transonic inviscid flow. The objective is to minimize the drag coefficient $C_d(\mathbf{x})$. The Mach number is $M_\infty = 0.734$, and the lift coefficient is set constant (by varying the angle of attack) at $C_l(\mathbf{x}) = 82.4$ l.c. (1 l.c. = 1 lift count = 1.0E−2). The cross-sectional area is constrained to be larger or equal to the value of the baseline. The design variables are the vertical coordinates of eight control points in a B-spline airfoil shape parameterization constrained to be within upper and lower bounds of 0.07 and −0.1, respectively (Fig. 1a).

The flow is simulated using computational fluid dynamics (CFD) where the high-fidelity model utilizes a fine mesh (obtained using a grid independence study). The low-fidelity models are the same as the high-fidelity one, but with coarser meshes and relaxed flow solver convergence criteria. The CFD models solve the compressible Euler equations on an O-type mesh (Fig. 1b) using the Stanford University Unstructured code[6]. The high-fidelity model, $\mathbf{f}(\mathbf{x})$, uses a 512 × 512 mesh, whereas the low-fidelity models, $\mathbf{c}_i(\mathbf{x})$, $i = 1,\ldots,6$, use the following discretization $\{\mathbf{c}_1$: 8 × 8$\}$, $\{\mathbf{c}_2$: 16 × 16$\}$, …, $\{\mathbf{c}_6$: 256 × 256$\}$, and a maximum number of solver iterations set to 300.

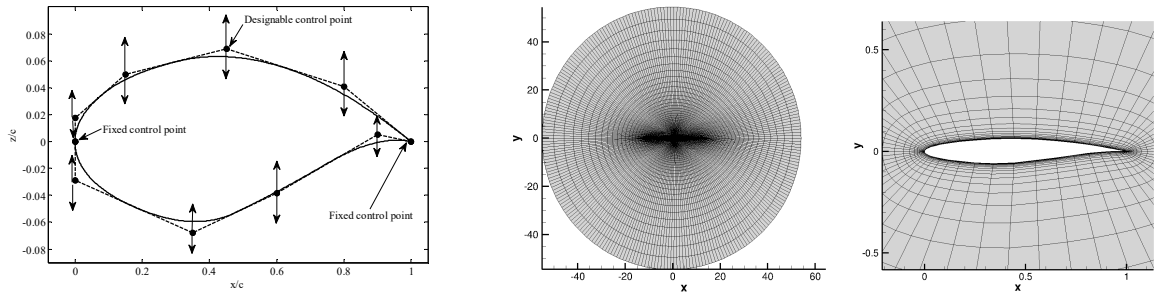

Figure 1. Airfoil description and computational mesh setup: (a) B-spline control points, (b) O-type mesh.

B. Statistical Analysis of the High- and Low-fidelity Model Correlations

The results of the statistical analysis are shown in Figs. 2 and 3. Note that the regression plots were not created for the two coarsest meshes (Mesh 1 and Mesh 2) because some of the simulations crashed for these meshes. It can be observed that the correlation between the low- and high-fidelity models is very good starting from Mesh 4 and up (here, we denote the high-fidelity model **f**(**x**) as Mesh 7), which is the first mesh for which the coefficient of determination exceeds the threshold value of 0.9.

C. Optimization Results

The results of the optimization runs are given in Table 1. All runs were successful, aside from the run using the second low-fidelity model. This run was not successful due to the low-fidelity model failing in completing the CFD simulation. Runs with low-fidelity models 4, 5, and 6 obtained nearly the same design, all yielding the lowest drag coefficients of approximately 10 d.c. (1 d.c. = 1 drag count = 1.0E–4). However, low-fidelity model 4 needed the least amount of time, around 1,328 min, which is approximately 329 min (–20%) less than with model 5, and approximately 92 min (–6.5%) less than with model 6. Although, model 4 needed almost twice as many function evaluations, the total optimization time is reduced because the average simulation time for model 4 is 1.1 min whereas the average simulation time for models 5 and 6 is 3.0 min. It should be noted that the quality of the final designs obtained with meshes 1 and 3 is poor compared with those obtained using meshes 4, 5, and 6, which confirms the importance of the appropriate selection of the low-fidelity model. According to the presented results, the optimum choice for the considered problem is Mesh 4, which is what was predicted by our statistical analysis.

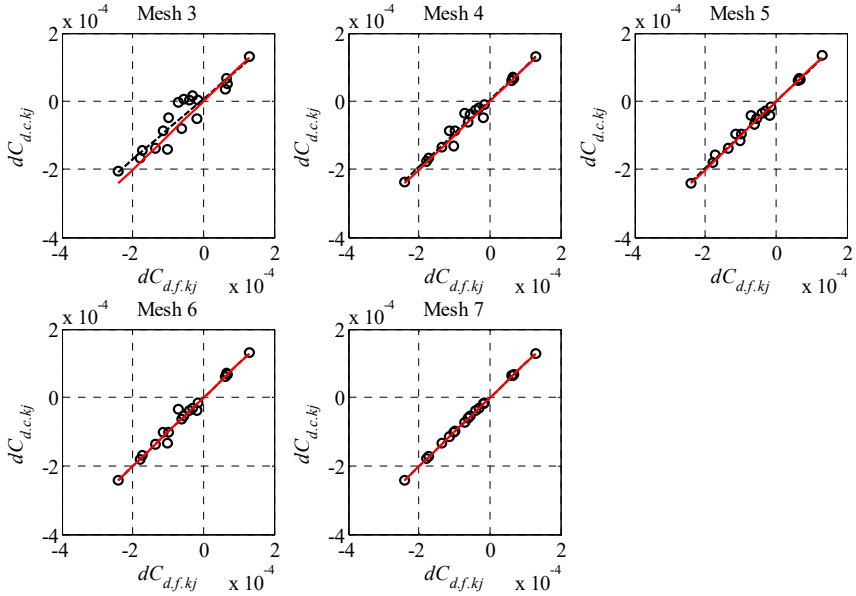

Figure 2. Scatter plots of $dC_{d.c.kj}$ versus $dC_{d.f.kj}$. The plots are created for 18 reference designs (six 3-design clusters), which gives 18 dC_d pairs. Solid line denotes regression line for the high-fidelity model data versus itself, whereas the dashed line denotes the regression line for the low-fidelity model data versus the high-fidelity model data. Note that the plots for Mesh 1 and Mesh 1 are not shown because some of the designs for these meshes did not simulate properly.

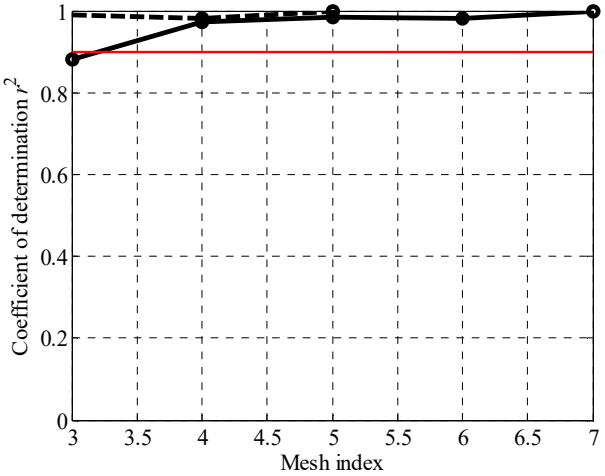

Figure 3. r^2 plots for the $\{dC_{d.f.kj}, dC_{d.c.kj}\}$ data sets versus model discretization level (here, marked as Mesh index 7 for the high-fidelity model, and lower numbers for low-fidelity models). Acceptable confidence level (0.9) is marked using a horizontal line. According to the plot, Mesh 4 seems to be the optimum low-fidelity model choice.

Table 1. Results of six optimization runs using the multi-point OSM algorithm with the high-fidelity model and each low-fidelity model. Optimization with the second low-fidelity model was unsuccessful.

Algorithm	Baseline	Multi-point Output Space Mapping					
Models	**f**	**f & c**$_1$	**f & c**$_2$	**f & c**$_3$	**f & c**$_4$	**f & c**$_5$	**f & c**$_6$
H(**f**(**x**)	0.0077	0.0027	–	0.0021	0.0010	0.0010	0.0010
h(**x**)	0.0000	0.0000	–	0.0000	0.0000	0.0000	0.0000
g(**x**)	0.0000	-0.0016	–	0.0000	-0.0016	-0.0019	-0.0021
C_d (d.c.)	76.71	26.78	–	20.79	9.75	9.98	9.92
C_l (l.c.)	82.40	82.40	–	82.40	82.40	82.40	82.40
A	0.0779	0.0795	–	0.0779	0.0795	0.0798	0.0800
N_c	–	66	–	323	1,033	524	452
N_f	1	2	–	2	4	2	2
t_c (min)	–	51.7	–	180.9	1,154.2	1,567.3	1,335.3
t_f (min)	32	63.8	–	103.2	129.5	66	65.1
t_{tot} (min)	32	125.2	–	292.56	1,318.3	1,647.1	1,410.1

IV. Conclusion

In the paper, a technique for automated selection of the low-fidelity model for variable-fidelity surrogate-assisted aerodynamic shape optimization has been proposed. The approach exploits statistical analysis of reference designs evaluated at various levels of structure discretization and aims at identifying the low-fidelity model setup that is as fast as possible and yet ensures sufficient correlation with the high-fidelity model. The proposed method is validated through optimization of airfoils in two-dimensional inviscid transonic flow.

References

[1]Forrester, A.I.J., and Keane, A.J., "Recent advances in surrogate-based optimization," *Progress in Aerospace Sciences*, Vol. 45, No. 1-3, 2009, pp. 50-79.

[2]Koziel, S., Cheng, Q.S., and Bandler, J.W., "Space mapping," *IEEE Microwave Mag.*, vol. 9, no. 6, pp. 105-122, Dec. 2008.

[3]Koziel, S. and Leifsson, L., "Knowledge-based airfoil shape optimization using space mapping," *30th AIAA Applied Aerodynamics Conference*, New Orleans, Louisiana, June 25-28, 2012.

[4]Conn, A.R., Gould, N.I.M., and Toint, P.L., *Trust Region Methods*, MPS-SIAM Series on Optimization, 2000.

[5]Koziel, S., "Multi-fidelity multi-grid design optimization of planar microwave structures with Sonnet," *International Review of Progress in Applied Computational Electromagnetics*, Tampere, Finland, 2010, pp. 719-724.

[6]Palacios, F., Colonno, M. R., Aranake, A. C., Campos, A., Copeland, S. R., Economon, T. D., Lonkar, A. K., Lukaczyk, T. W., Taylor, T. W. R., and Alonso, J. J., "Stanford University Unstructured (SU^2): An open-source integrated computational environment for multi-physics simulation and design," AIAA Paper 2013-0287, 51st *AIAA Aerospace Sciences Meeting and Exhibit*, Grapevine, Texas, USA, 2013.